Supplement of Atmos. Chem. Phys., 21, 17995–18010, 2021
https://doi.org/10.5194/acp-21-17995-2021-supplement

Atmospheric Chemistry and Physics
Open Access
EGU

Supplement of

Measurement report: Fast photochemical production of peroxyacetyl nitrate (PAN) over the rural North China Plain during haze events in autumn

Yulu Qiu et al.

Correspondence to: Zhiqiang Ma (zqma@ium.cn)

Method S1. Calculation of HO_x production rates through three pathways

Photolysis of O_3, HONO and HCHO are usually considered as the three major HO_x sources during the daytime. Photolysis of HONO can directly produce OH radical and the production rate of HO_x ($P[HO_x]_{HONO}$) is the product of photolysis rate and HONO concentration.

$$HONO + h\nu \rightarrow OH + NO \quad (1)$$

$$P[HO_x]_{HONO} = J_{HONO} \times [HONO] \quad (2)$$

O_3 photolysis can produce excited singlet oxygen atom ($O(^1D)$), and $O(^1D)$ collides with N_2 or O_2, quenching to its ground state or reacts with H_2O to generate two OH radicals

$$O_3 + h\nu \rightarrow O(^1D) + O_2 \quad (3)$$

$$O(^1D) + [M] \rightarrow O + M \quad (4)$$

$$O(^1D) + H_2O \rightarrow 2OH \quad (5)$$

Following the estimation method in Seinfeld and Pandis (2006), the HO_x production rate by O_3 photolysis could be derived by

$$P[HO_x]_{O_3} = \frac{2J_{O_3} \times k_4 \times [H_2O] \times [O_3]}{[M] \times k_3} \quad (6)$$

Photolysis of HCHO directly produces H and HCO. Because of the rapid reaction between HCO (H) and O_2, HCHO photolysis could be represented as

$$HCHO + h\nu + 2O_2 \rightarrow 2HO_2 + CO \quad (7)$$

and the production rate of HO_x is calculated by

$$P[HO_x]_{HCHO} = 2J_{HCHO} \times [HCHO] \quad (8)$$

Method S2. Cacluation of PA radical concentration and PAN production rate

In this study, we estimate PA radical concentration and also obtain PAN production rate in another way. As shown in Section 3, PA radical is usually formed through the reaction between CH_3CHO and OH (9), and the major sinks of PA are reactions between NO_2 (10) and NO (11).

$$CH_3CHO + OH \xrightarrow{O_2} PA + H_2O \quad (9)$$

$$PA + NO_2 \rightarrow PAN \quad (10)$$

$$PA + NO \rightarrow CH_3 + NO_2 + CO_2 \quad (11)$$

Since PA is rather reactive, it may reach steady state and thereby we assume that the rate of PA formation is equal to the rate of loss. Thus, PA radical concentration can be calculated by:

$$[PA] = \frac{k_1[CH_3CHO][OH]}{k_2[NO_2]+k_3[NO]} \quad (12)$$

where $k_1=5.55\times10^{-12}\exp(311/T)$, $k_3=8.1\times10^{-12}\exp(270/T)$, $k_2=\left[\frac{k_0[M]}{1+\frac{k_0[M]}{k_\infty}}\right]F^{\left[\frac{1}{1+\left[\log_{10}\left(\frac{k_0[M]}{k_\infty}\right)\right]^2}\right]}$, $k_0=9.7\times10^{-29}(T/300)^{-5.6}$, $k_\infty=9.3\times10^{-12}\ (T/300)^{1.5}$, F=0.6, following the reaction coefficients in Seinfeld and Pandis (2006). OH concentration is assumed to be with a maximum value of 3.0×10^6 molec cm^{-3} at noon, which is consistent with Lu et al. (2019). Therefore, PAN production rate can be estimated by $k_2[PA][NO_2]$.

Table S1. Detailed parameters of instruments used in this study.

Species	Instruments	Time resolution	Detection limit	Calibration frequency
PAN	GC-ECD	5 mins	20 ppt	monthly
VOCs	PTR-ToF-MS	5 mins	-	monthly
HONO	LOPAP	1 min	10 ppt	weekly
O_3	TE 49i	1 min	0.5 ppb	monthly
NO_x	TE 42i	1 min	50 ppt	monthly
CO	Picarro, G2401	2 secs	40 ppb	monthly
$PM_{2.5}$	TEOM 1405	5 mins	0.1 μg/m³	-
Photolysis (*J*)	PFS-100	1 min	-	quarterly

Table S2. Comparisons of PAN levels in recent studies in China with results in this study.

Location	Site type	Period	Conc. (ppb)	Reference
Jinan, Shandong, China	Urban NCP	Nov 2015−Jul 2016	1.89±1.42	Liu et al. (2018)
Tianjin, China	Suburban NCP	Sep 5−28, 2018	0.93±0.57	Qiu et al. (2019a)
PKU, Beijing, China	Urban NCP	Jun−Jul, 2014	1.5	Zhang et al. (2017)
Wangdu, Hebei, China	Rural NCP	Jun−Jul, 2014	1.7	Zhang et al. (2017)
Beijing, China	Suburban NCP	Jan−Feb, 2016	1.04	Zhang et al. (2019)
CS, Chongqing, China	Urban site	Aug 25−Sep 10, 2015	2.05	Sun et al. (2020)
NQ, Chongqing, China	Suburban site	Aug 25−Sep 10, 2015	1.08	Sun et al. (2020)
Xiamen, Fujian, China	Suburban site	Jan–Dec, 2018	0.55	Hu et al. (2020)
Hongkong, China	Suburban site	Oct–Nov, 2016	0.63±0.05	Zeng et al. (2019a)
Ziyang, Sichuan, China	Suburban site	Dec, 2012	0.55	Zhu et al. (2018)
Central Tibetan Plateau, China	Background site	Aug17−24, 2011 May 15−Jul 2012	0.36 0.44	Xu et al. (2018)
SDZ, Beijing, China	Rural NCP	Oct, 2020	1.11±0.88	This study

Table S3. Comparisons between estimated reaction rates through HO_2+NO and HO_2+HO_2 during pollution days at the SDZ site.

	k[a] (cm^3 $molec^{-1}$ s^{-1})	HO_2[b] (molec cm^{-3})	NO or HO_2 (molec cm^{-3})	Reaction rates[c] (molec cm^{-3} s^{-1})
HO_2+NO	8.4×10^{-12}	~10^8	7.1×10^9 for NO	~6×10^6
HO_2+HO_2	3.3×10^{-12}	~10^8	~10^8 for HO_2	~3.3×10^4
R1/R2	2.5	1	~71	~1.8×10^2

[a]. k denotes the reaction coefficients of HO_2+NO (k_{NO}) and HO_2+HO_2 (k_{HO2}).

[b]. The HO_2 concentration is assumed to be with a magnitude of 10^8 molec cm^{-3} , which is consistent with Tan et al. (2018).

[c]. The reaction rates of HO_2+NO and HO_2+HO_2 are calculated by k_{NO} [HO_2][NO] and k_{HO2} [HO_2][HO_2], respectively.

Table S4. Comparisons of HCHO levels in recent studies in China with our result.

Location	Site type	Period	Conc. (ppb)	Reference
Beijing, China	Suburban NCP	Summer, 2008	11.17 ± 5.32	Yang et al. (2018)
Beijing, China	Suburban NCP	October, 2006	7.49	Pang et al. (2009)
Beijing, China	Urban NCP	Summer, 2013	11.4 ± 5.6	Rao et al. (2016)
		Winter, 2014	5.5 ± 3.9	
Beijing, China	Urban NCP	Summer, 2015	6.9 ± 2.9	Qian et al. (2019)
		Summer, 2018	8.5 ± 2.1	
		Winter, 2017	3.2 ± 2.4	
Beijing, China	Urban NCP	August, 2006	29.2 ± 12.1	Duan et al. (2012)
Beijing, China	Urban NCP	December, 2016	18.3 ± 7.2	Sheng et al. (2018)
Beijing, China	Suburban NCP	Autumn, 2005	15.8 ± 9.7	Zhang et al. (2012)
		Autumn, 2008	5.9 ± 3.2	
		Autumn, 2009	8.3 ± 5.8	
Beijing, China	Urban NCP	November, 2014	14.2 ± 13.8	Zhou et al. (2019)
		July, 2015	12.8 ± 4.8	
Wangdu, China	Rural NCP	Nov−Dec, 2017	3.7	Wang et al. (2020)
Shenzhen, Guangdong, China	Urban site	Spring, 2016	3.4 ±1.6	Wang et al. (2017)
		Summer, 2016	5.0 ± 4.4	
		Autumn, 2016	5.1 ± 3.1	
		Winter, 2016	4.2 ± 2.2	
Wujiasha, China	Suburban site	August, 2016	2.1 ± 0.2	Zeng et al. (2019b)
Ziyang, Sichuan, China	Urban site	August, 2016	2.2 ± 0.4	
Hankou, Hubei, China	Roadside site	August, 2016	3.4 ± 0.5	
Nanning, Guangxi, China	Urban site	Oct 2011−Jul 2012	5.6 ± 2.8	Guo et al. (2016)
Mount Tai, Shandong, China	Background site	Summer, 2014	3.5 ± 1.0	Yang et al. (2017)
Wuhan, Hubei, China	Suburban site	Feb, Apr, July, Oct of 2017	3.4 ± 2.0	Yang et al.(2019)
Guangzhou, Guangdong, China	Urban site	July, 2006	7.6 ± 3.7	Ling et al. (2017)
SDZ, Beijing, China	Rural site	Oct., 2020	4.6 ± 3.8	This study

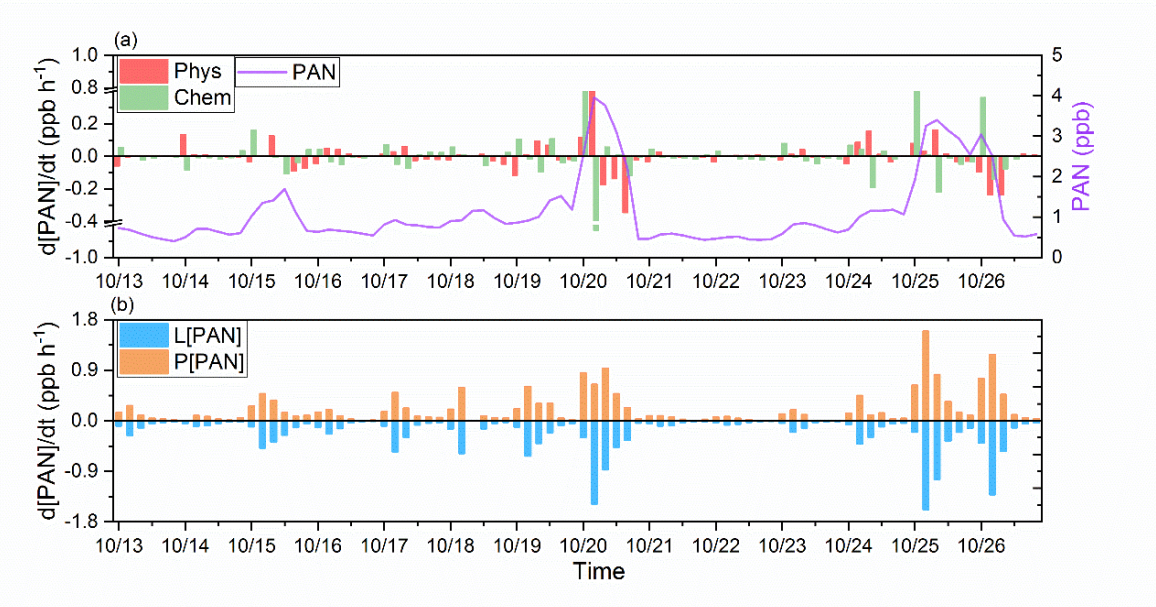

Figure S1. (a) Changes in PAN concentrations every four hours due to physical (Phys) and chemical (Chem) processes during the observation period at the SDZ site. (b) Chemical change rates of PAN due to chemical production (P[PAN]) and loss (L[PAN]) rates every four hours during the observation period at the SDZ site.

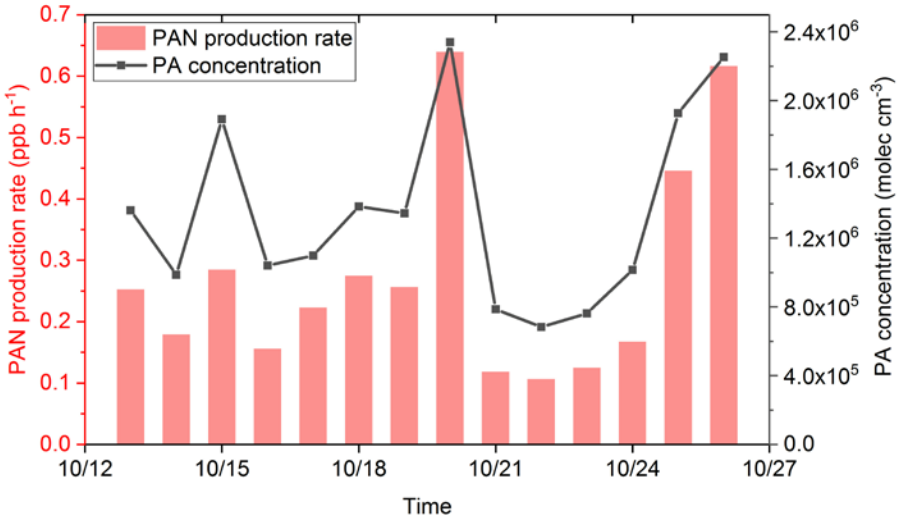

Figure S2. Time series of calculated PAN production rates (ppb h^{-1}) through reaction between PA radical and NO_2 and PA concentrations (molec cm^{-3}) at the SDZ site on the mornings of the observation period.